THE JOURNAL OF PHYSICAL CHEMISTRY C
A JOURNAL OF THE AMERICAN CHEMICAL SOCIETY

pubs.acs.org/JPCC

Article

Nb-Implanted BaO as a Support for Gold Single Atoms

Debolina Misra* and Satyesh K. Yadav

Cite This: https://doi.org/10.1021/acs.jpcc.1c07859

Read Online

ACCESS | Metrics & More | Article Recommendations

ABSTRACT: Using first-principles modeling based on density functional theory, we show that oxides implanted with transition metals (TMs) can act as an ideal support for Au single atoms, preventing agglomeration. In our previous work, we have shown that TM atoms, if implanted in oxides such as BaO, are stable as interstitial in various charge states, and the stability can be achieved by transferring the excess charge to an acceptor level close to valence band maximum (VBM). Taking Nb as the dopant, implanted in BaO, we show that single-atom Au having its Fermi level close to the VBM of BaO is able to accept charge from the dopant. This charge-transfer process between Nb and Au can result in the strong binding of Au atoms on the doped BaO support. We also show that these charged Au atoms repel each other and prefer to remain atomically dispersed, preventing cluster formation. Substitutional doping of TMs has earlier been reported to bind Au atoms. However, in this work, we show that an interstitially doped TM can bind more Au atoms; for example, five Au atoms can be anchored per Nb dopant present in the BaO interstitial compared to three Au atoms when Nb is doped at the substitutional site. Shedding light on the benefit of interstitial implantation of TM dopants in oxides and their role in stabilizing single atoms of noble metals through dopant to adatom charge transfer, this work paves the way for an altogether new technique of stabilizing noble metal single atoms on TM-doped oxides.

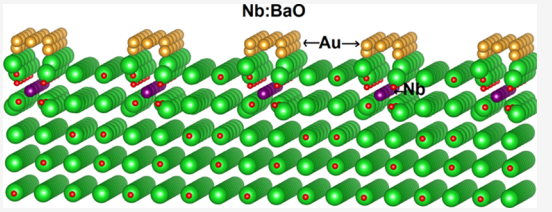

INTRODUCTION

In spite of the tremendous growth in designing non-noble materials for catalysis, noble metals are still at the heart of catalysis research due to their highest catalytic activity.[1] Noble metal nanoparticles (NPs) are often used due to the large surface-to-volume ratio and the higher concentration of the undercoordinated surface sites they expose compared to larger particles with more extended surfaces. Nevertheless, the high cost and low abundance of noble metals still significantly hinder the use of such NPs as catalysts.[2,3] Single-atom catalysts (SACs), which consist of atomically dispersed metal atoms on a support, are promising solutions to reduce this cost. They maximize the surface-to-volume ratio, which can potentially lead to a way more efficient use of the noble metals and thus decrease the cost of catalyst fabrication.[4,5] Despite the existing challenges in the preparation of stable and active SACs, the last decade has seen several successful strategies for fabricating a promising SAC prototype.[6−8]

Nevertheless, atomically dispersed metals are often unstable against agglomeration into larger metal NPs.[8−10] Efficient SACs must therefore be catalytically active and resistant to sintering, both of which strongly depend on intricate metal−support interactions. Doped oxides act as very effective supports for catalysts. The dopant first changes the electronic structure of the host and can cause a charge transfer, which is not only limited to the direct interaction of the dopant and its nearby host atoms but can also be extended to the adsorbate situated on the surface of the host lattice.[11] Such processes of charge transfer between the impurity, host lattice, and adsorbate are at the heart of heterogeneous catalysis where charge transfer to a proper adsorbate on the oxide surface can reduce the barrier of a chemical reaction. Recently, it has been shown that for a charge transfer to take place between a dopant and an adsorbate, a direct interaction is not always necessary.[12] Some earlier studies have revealed that the adsorption properties of gold and its growth pattern strongly depend on the charge transfer to gold atoms, which in turn depend on the nature of the dopant and the host lattice.[13,14] For example, Mo transfers charge to Au in CaO and MgO and alters its growth pattern on the oxide surface. However, the presence of Cr in both the oxides resulted in no charge transfer between gold atoms and Cr.[15]

To stabilize single-atom Au, all the previous studies have focused on substitutional doping of oxides with transition metals (TMs). Here, we conclusively show that interstitially doped oxides can act as a better support as TMs at the interstitial site can transfer more charge than at the substitutional site. We use density functional theory (DFT) to show that (1) Nb prefers to be in the 5+ charge state and

Received: September 5, 2021
Revised: November 14, 2021

occupy the interstitial site in BaO, (2) doped Nb transfers excess electrons to the Au atoms adsorbed on the surface and binds them strongly, and (3) Au atoms anchored to the support repel each other and resist cluster formation.

COMPUTATIONAL DETAILS

All the spin-polarized DFT calculations were performed employing the projector-augmented wave (PAW) method[16] and a plane wave basis set with an energy cut-off of 500 eV, as implemented in Vienna *Ab Initio* Simulation Package (VASP).[17,18] Generalized gradient approximation (GGA) was used to treat the electronic exchange and correlation, employing the Perdew, Burke, and Ernzerhof (PBE) functional.[19] A k-point mesh of $4 \times 4 \times 4$ was used for achieving converged results within 10^{-4} eV per atom. All the structures were fully relaxed using the conjugate gradient scheme, and relaxations were considered converged when forces on each atom were smaller than 0.02 eV/Å. The calculation of density of states (DOSs) was performed using a linear tetrahedron method with Blochl corrections[20] and a denser k-grid. For the bulk calculations, a cubic super cell containing 32 formula units of BaO was doped with Nb in all their possible charge states, which results in a dilute limit (3.1%) of doping.

RESULTS

Stability and Preferred Charge State of Nb Dopant in BaO. First, we attempt to understand the charge state of Nb when doped in BaO and its electronic structure to ascertain its potential to transfer charge to Au. The ionic radii of Nb in a six-coordinated environment are 0.70, 0.68, and 0.64 Å in +3, +4, and +5 charge states, respectively, while the ionic radius of Ba is 1.35 Å. Our prediction model[21] suggests that Nb will be stable as an interstitial in bulk BaO. We indeed find that Nb is stable at the interstitial site. We calculate the defect formation energy E_f^q[22−25] of Nb in bulk BaO as a function of electronic chemical potential, μ, using the following equation:

$$E_f^q = E_D^q - E_B - \eta + q(\mu + E_{ref} + \Delta V) + E_{corr}^q \quad (1)$$

Here, E_D^q and E_B are the total energies of the defect supercell with charge q and the defect-free host supercell, respectively. η is the chemical potential of the TM atom species. The "−" sign indicates the addition of defects in the host. E_{ref} is a suitable reference energy, taken to be the valence band maximum (VBM), and ΔV is the correction to realign the reference potential of the defect supercell with that of the defect-free supercell.[26] E_{corr}^q is the correction to the electrostatic interaction and the finite size of the supercell. In this work, only the first-order monopole correction has been taken into account.

The defect formation energy of Nb in bulk BaO as a function of electronic chemical potential is shown in Figure 1. Nb is stable in a single charge state (+5) for the entire range of electronic chemical potentials (μ) studied. Here, μ varies from VBM up to the band gap of the host oxide obtained from our DFT calculations. As we intend to use Nb-doped BaO as a support for single-atom Au, we explored the following: (1) change in the Fermi-level position of doped BaO with different charge states of Nb and (2) stability of Nb in BaO at various depths from the surface.

The DOS for Nb-doped bulk BaO is shown in Figure 2. For all the charge states of Nb except +5, the Fermi level lies in the antibonding state, which indicates that these states are not

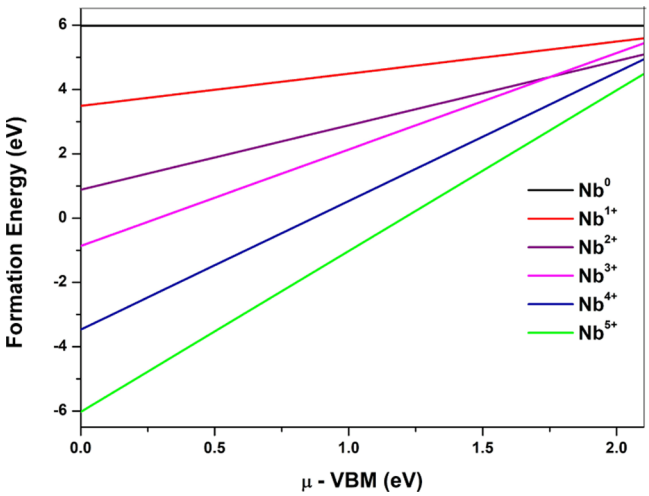

Figure 1. Defect formation energy for the neutral and charged Nb interstitial in bulk BaO as a function of electronic chemical potential μ.

stable. The Fermi level lies at the VBM only for the +5 charge state of Nb in BaO, which suggests that this state is the most stable one. The change in the Fermi level position for different charge states of Nb is similar to substitutionally doped oxides, generally used to stabilize single atoms.[12,15] We can expect that the five valence electrons of Nb can be transferred to an acceptor when BaO is doped with Nb.

The stability of Nb interstitials at various depths from the surface of BaO has been investigated in order to trace its most preferred position. A five-layer-thick BaO slab containing {001} surfaces (known to be one of the most stable surfaces of BaO) is used to model the surface. The in-plane dimension of supercell is 2×2 units of BaO with a 12 Å vacuum along the [001] direction. The atoms in the bottom two layers of the slab are frozen to their bulk positions in all our calculations.

Nb in different layers (subsurface, sub-subsurface, and on surface O-top and hollow sites) of the BaO{001} surface is shown in Figure 3. The relative energies between all these three configurations for both neutral Nb and Nb in the +5 charge state are listed in Table 1.

From Table 1, it can be seen that the subsurface layer is energetically the most preferred layer for Nb interstitial in both neutral and +5 charge states. However, the most important observation one can make from this calculation is, although Nb neutral is stable in the subsurface layer, the difference between configurations with Nb occupying the subsurface interstitial and on surface O-top site is very small (0.18 eV). Hence, under high temperature, neutral Nb can easily escape from the subsurface layer and can occupy the surface O-top site. The Nb-occupying surface O-top site will further lead to the highly stable Nb_2O_5 oxide formation as the formation enthalpy for Nb_2O_5 is −9.84 eV per Nb atom.[27] However, the scenario changes drastically once Nb reaches its most preferred valence state +5. The difference in energy between slabs containing Nb in the subsurface and occupying O-top site is nearly 10 eV. This huge difference in energy will prevent Nb^{5+} from escaping the oxide subsurface layer and forming Nb_2O_5. The stability of Nb^{5+} in the subsurface BaO slab and the huge energy difference between Nb^{5+} at the subsurface and surface O-top sites provide a unique opportunity to use Nb-doped BaO as a support for Au single atoms where transfer of excess charge

https://doi.org/10.1021/acs.jpcc.1c07859
J. Phys. Chem. C XXXX, XXX, XXX−XXX

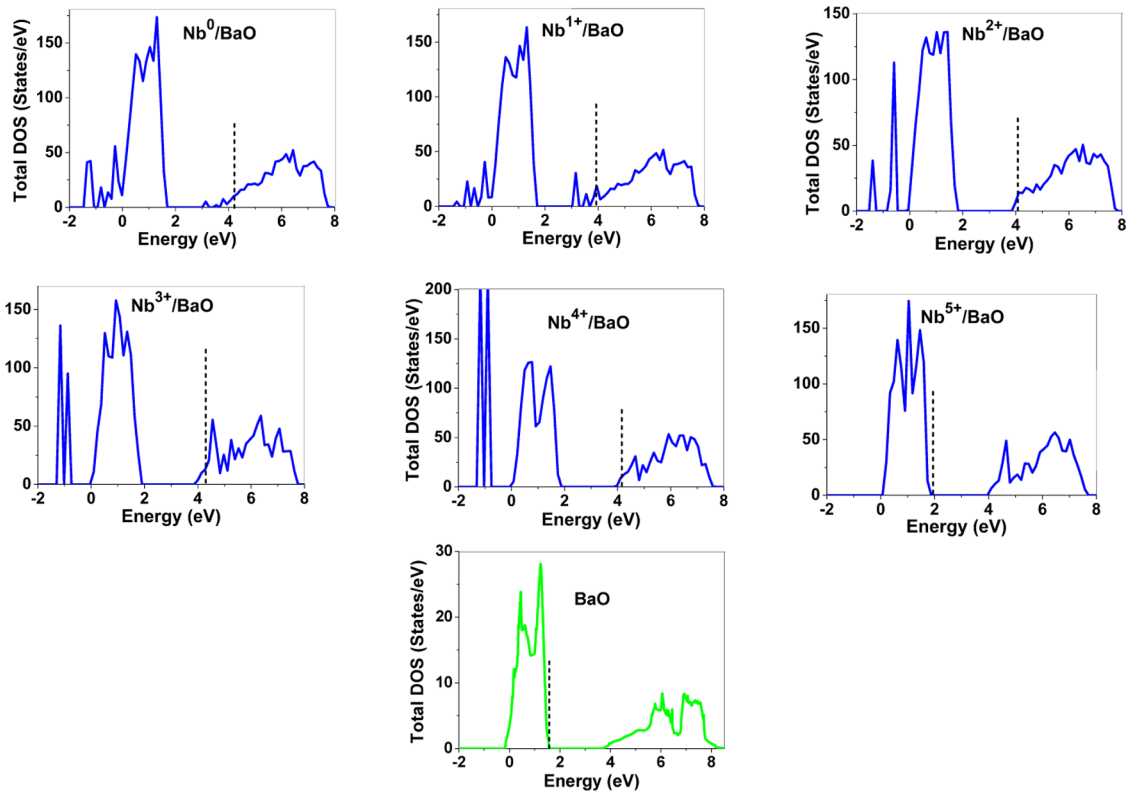

Figure 2. Total DOS of Nb-doped BaO and pure BaO. The vertical dashed line indicates the Fermi level.

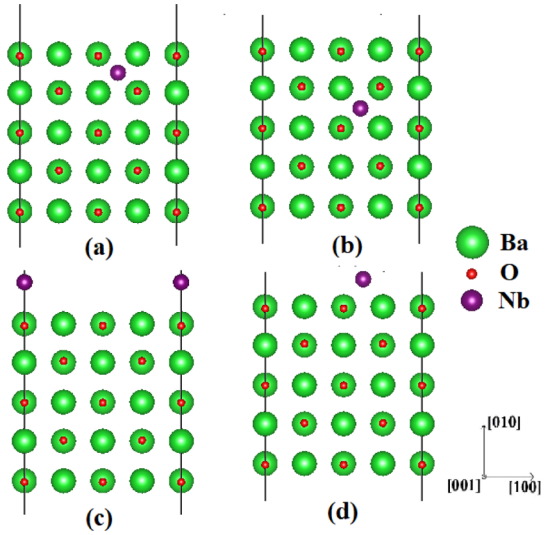

Figure 3. BaO{001} surface with Nb in different layers; Nb at the (a) subsurface and (b) sub-subsurface and on surface (c) O-top and (d) hollow sites.

Table 1. Relative Energy of BaO{001} Surfaces Containing Nb at Different Layers

	relative energy (eV)	
position	Nb^0	Nb^{5+}
subsurface (Figure 3a)	0.00	0.00
sub-subsurface (Figure 3b)	1.76	1.22
on surface O-top (Figure 3c)	0.18	9.58
on surface hollow (Figure 3d)	1.50	6.09

from Nb to Au can cause a strong binding of Au on the support.

Adsorption of Au on Nb-Doped BaO Surface. *Preferred Binding Site of a Single Au Adatom.* The relaxed supercell that we used to calculate the energy of Nb doped at the subsurface site has been taken to understand the adsorption of Au. While calculating the Au adsorption on one side of the doped BaO surface, necessary dipole corrections were included. Keeping in mind the hollow and O-top sites as the possible binding sites for noble metal atoms on a pure BaO slab, we explored various possible binding sites for a Au atom on an Nb-doped BaO slab. The potential binding sites are named as Nb-top, near-Nb O-top (when the binding oxygen atom is a part of the oxygen tetrahedra formed around Nb), and far O-top (when the binding oxygen atom is not a part of the tetrahedra formed around Nb) sites as shown in Figure 4. The relative energies of Au single atoms on these sites are listed in Table 2. We also explored hollow, Ba-top, and bridge sites; however, for the hollow site, the Au atom ends up at the near-Nb O-top site, and in both the latter cases, the Au atom ended up on the neighboring O-top sites, indicating that these sites are not the preferred binding sites for Au atoms on the Nb-doped BaO support. Our calculations revealed that the Au atom binds most strongly on the near-Nb O-top sites. For Au to get adsorbed on the far O-top sites, it costs almost 0.29 eV more energy compared to the near-Nb O-top sites. The surface Nb site is also higher in energy compared to the near Nb O-top sites. Hence, the oxygen atom near Nb acts as the most preferred and strongest binding site for Au adsorption on Nb-doped BaO.

Stability of Au Atoms. The stability of Au atoms on pure and Nb-doped BaO supports was examined in terms of Au

https://doi.org/10.1021/acs.jpcc.1c07859
J. Phys. Chem. C XXXX, XXX, XXX−XXX

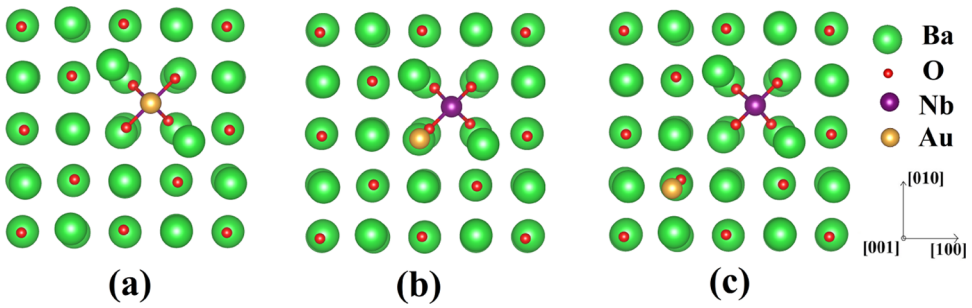

Figure 4. Possible binding sites of a single Au atom on the Nb-doped BaO{001} surface. Au occupies the (a) Nb top, (b) near-Nb O-top, and (c) far O-top sites.

Table 2. Relative Energies of a Au Single Atom Adsorbed at Different Sites on the Nb-Doped BaO{001} Surface

binding site	relative energy (eV)
near-Nb O-top (Figure 4b)	0.00
Nb top (Figure 4a)	0.09
far O-top (Figure 4c)	0.29

adsorption energy for one, two, three, four, and five Au atoms using the equation

$$E_{ads} = E_{sup+Au} - E_{sup} - nE_{Au} \quad (2)$$

where E_{sup+Au}, E_{sup}, and E_{Au} refer to the energies of the support (pure or Nb-doped BaO) with Au atoms, only support without Au, and energy of a Au single atom, respectively, and n is the number of Au atoms adsorbed on the support. For adsorption of three and more (four and five) Au atoms on the Nb-doped BaO{001} surface, the adsorption sites are chosen in such a way that two Au atoms occupy the near-Nb O-top sites (strongest binding site), one Au atom occupies the Nb-top site (the second most preferred binding site for Au), and the rest Au atoms occupy the surface O-top sites. The adsorption energies for Au single atoms on pure and Nb-doped BaO supports are listed in Table 3. It is evident from Table 3 that compared to the bare BaO surface, the Nb-doped BaO surface binds a single Au atom substantially well. The adsorption energy is almost 2 eV stronger when BaO is doped with Nb.

This strong adsorption of the Au atom could be due to a charge transfer to Au. We have calculated the excess charge (the difference in charge on the Au atom and the number of valence electrons) on the Au atom using the Bader decomposition scheme,[28−30] and the results are listed in Table 3. Our calculations revealed that there is a transfer of almost one electron from Nb to Au, causing the Au atom to bind strongly on the support. Transfer of charge to Au is significantly low in the case of pure BaO support. For an Nb-doped BaO slab, the Au atom acts as an acceptor of charge-accepting excess electrons from Nb, and the charge-transfer process continues when the number of adsorbed Au atoms is increased until a maximum of five Au atoms are adsorbed on the slab.

Cluster Formation of Au Atoms. In order to understand the stability of the adsorbed Au atom against segregation, we study the interaction of two, three, four, and five Au atoms adsorbed on pure BaO and Nb-doped BaO surfaces. We find that the charged Au atoms on the Nb-doped BaO support resist clustering, one of the bottlenecks in fabricating SACs.

Figure 5 shows the optimized structures for two Au atoms (a) on two different O-top sites and (b) together on the same O-top site forming a Au_2 cluster on the pure BaO{001} surface, along with their relative energies. Comparison between these two arrangements revealed that formation of a Au_2 cluster is more energetically favorable on a pure oxide slab with a d_{Au-Au} separation of 2.54 Å, smaller than 2.78 Å reported for Au_4 clusters .[31] A similar trend has been observed for three, four, and five Au atoms on the pure BaO slab where Au atoms show the tendency to form clusters with an average Au−Au bond length of 2.65, 2.51, and 2.74 Å, respectively. Hence, the Au atoms bound on the pure BaO slab are prone to form larger particles.

On the other hand, for an Nb-doped BaO slab, a completely opposite trend has been observed. The Au atoms anchored on the doped oxide surface preferred to remain atomically dispersed and resist cluster formation. Figure 6 depicts the possible configurations taken by two Au atoms on the Nb-doped BaO slab: the optimized structures for two Au atoms (a) on two near-Nb O-top sites and (b) one Au atom on the near-Nb O-top site and the other one on the far O-top site. Figure 6c shows the initial structure of two Au atoms adsorbed on the same O-top sites. The relative energies between these configurations are also mentioned in Figure 6. We find that Figure 6a shows the most favored configuration for two Au

Table 3. Adsorption Energy (E_{ads}), Bader Charge q, and Average Au−Au Bond Length (d_{Au-Au}) for Au Atoms on Nb-Doped and Pure BaO{001} Surfaces and Binding Energy (Per Au Atom) ($B.E._{Au}$) and Au−Au Bond Length (d_{Au-Au}) for Au Atoms in Free-Standing Au Clusters

	Nb-doped BaO{001}			pure BaO{001}			free-standing Au cluster	
no. of Au atoms	E_{ads} (eV)	q (e)	d_{Au-Au} (Å)	E_{ads} (eV)	q (e)	d_{Au-Au} (Å)	$B.E._{Au}$ (eV/atom)	d_{Au-Au} (Å)
1	−3.83	−0.84		−1.88	−0.40			
2	−3.78	−0.83	4.64	−2.47	−0.21	2.54	−1.35	2.51
3	−4.10	−0.79	2.83	−2.67	−0.24	2.65	−1.38	2.55
4	−3.95	−0.74	2.81	−2.37	−0.26	2.51	−1.72	2.68
5	−3.91	−0.73	2.82	−1.80	−0.23	2.74	−1.85	2.62

https://doi.org/10.1021/acs.jpcc.1c07859
J. Phys. Chem. C XXXX, XXX, XXX−XXX

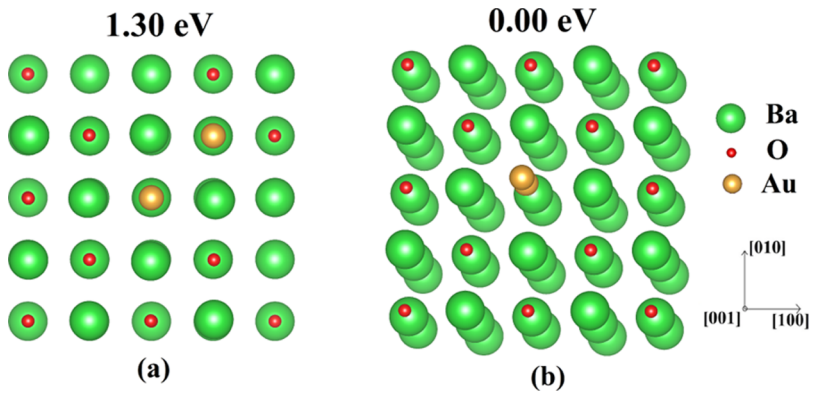

Figure 5. Two Au atoms on the pure BaO{001} surface and their relative energy.

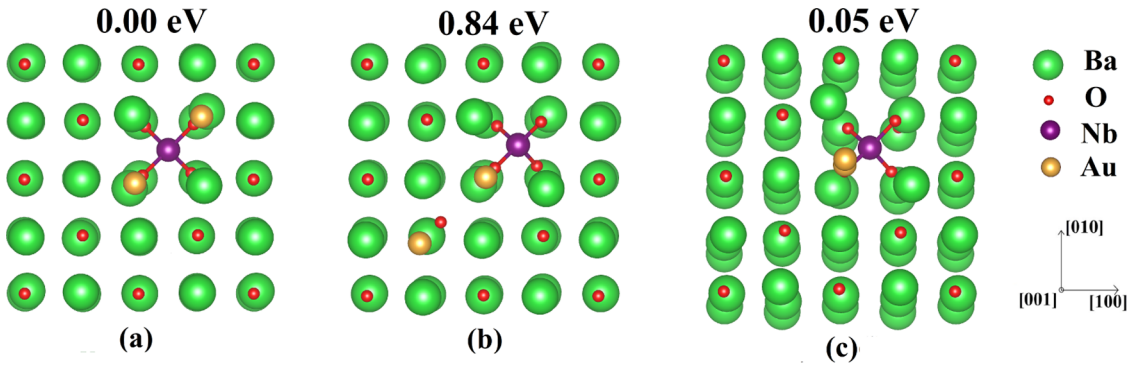

Figure 6. Various possible arrangements of two Au atoms on the Nb-doped BaO{001} support with their relative energies.

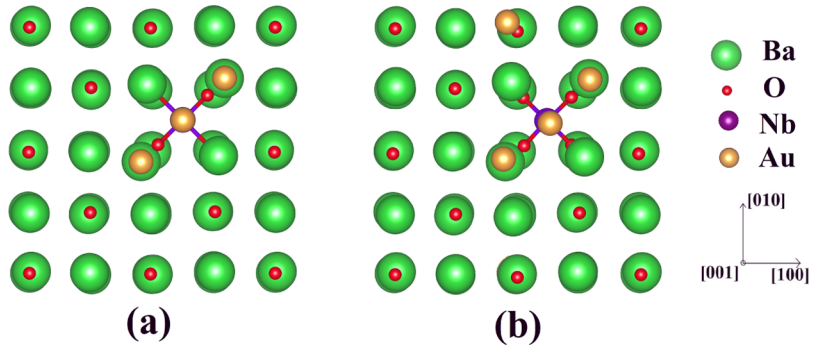

Figure 7. Adsorption of (a) three and (b) four Au atoms on the Nb-doped BaO{001} support.

atoms on the Nb-doped BaO support with a bond length of 4.64 Å. The third configuration (6c) is not stable, and after optimization, it comes to configuration (6a). This clearly shows that the Nb-doped BaO{001} surface acts as an agglomeration-resistant support for Au SAs. For more than two Au atoms on Nb-doped BaO, the Au atoms seem to move away from each other, indicating that they resist forming a larger particle and prefer to remain dispersed in the form of single atoms. For all the cases, the average Au−Au bond lengths (Table 3) are higher than the bond lengths reported for Au clusters of similar size[31] or for free Au clusters supported by ligands.[32] Hence, it is evident that Nb doping not only binds Au SAs more strongly but also prevents cluster formation of the SAs.

To show that Au atoms indeed prefer to remain atomically dispersed on the doped support, we have, in addition, calculated the binding energy per Au atom ($B.E._{Au}$) and the Au−Au separation in free-standing Au clusters containing two, three, four, and five Au atoms. For all the cluster calculations, the Au atoms were placed in a large cubic cell of 15 Å side length, and we started with structures of Au clusters available in the literature.[33,34] The structures were then fully relaxed. The $B.E._{Au}$ in a cluster is calculated using the relation

$$B.\ E._{Au} = (E_{Au_n} - nE_{Au})/n \quad (3)$$

where E_{Au_n} and E_{Au} denote the energies of the Au cluster containing n Au atoms and of a single Au atom, respectively. For all the Au_n clusters (n = 2, 3, 4, and 5), the $B.E._{Au}$ values along with the minimum Au−Au bond length in the cluster are enlisted in Table 3. A comparison between the energy required for Au adsorption on the BaO supports with the binding energy of Au atoms in the Au cluster reveals that instead of forming clusters, it is more preferred for Au atoms to get adsorbed and remain atomically dispersed on the Nb-doped BaO support. However, Au SAs are prone to cluster formation

https://doi.org/10.1021/acs.jpcc.1c07859
J. Phys. Chem. C XXXX, XXX, XXX−XXX

on a pure BaO support. A comparison of Au−Au bond lengths for Au atoms on the pure BaO support with that in Au clusters is also supportive of the fact that Au prefers to form a cluster with an average Au−Au bond length being smaller than that in the free-standing Au clusters for all the cases we studied. On the other hand, for Au atoms (2−5) on the Nb-doped BaO support, the Au atoms prefer to maintain a separation always higher than what is observed in free-standing Au clusters, indicating that the Au atoms remain in the atomically dispersed form as already evident from our calculations discussed above (Figures 7 and 8).

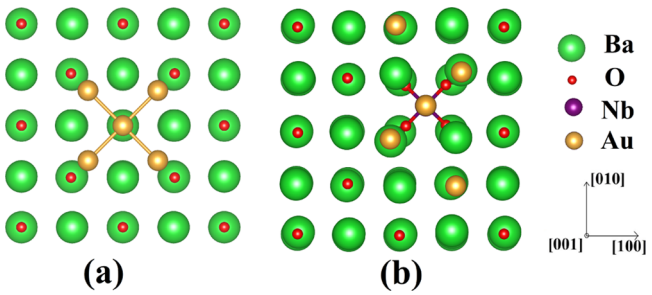

Figure 8. Arrangement of five Au atoms on (a) pure and (b) Nb-doped BaO{001} surfaces.

Electronic Structure. To explain why charge transfer takes place between Nb and Au atoms, we calculate DOS for (a) pure BaO, (b) one Au atom adsorbed on pure BaO, (c) Nb-doped BaO, and (d) one Au, (e) two Au, and (f) five Au atoms adsorbed on Nb-doped BaO{001} surfaces. Atom-resolved DOS are shown in Figure 9; for Au atoms, only 6s states are shown. Being an insulator, the pure BaO{001} surface shows no defect states in the band gap region, and a single-atom Au adsorbed on pure BaO has its 6s orbital half-filled. Once Nb is doped in BaO, the midgap states, mostly carrying the d-orbital signature of Nb, appear in the band gap region of BaO. These mid gap states ease the charge transfer between Nb and Au. For BaO doped with Nb, the highest occupied level of the system is pushed to CBM of BaO. Once one or two single atoms of Au get adsorbed on the Nb-doped BaO support, the highest occupied level of the system remains in the CBM with both the 6s states of Au now being occupied and degenerated, which is attributed to the charge transfer from Nb to Au. It is only after the adsorption of five Au atoms, the highest occupied level comes down to the VBM, indicating that all the excess five electrons are transferred to Au from Nb. Unlike the pure BaO support, the charge transfer between Nb and Au is evident for the doped one. A single Au atom can accommodate one extra electron from Nb in its s orbital, and this charge-transfer process continues till all the five Au atoms are adsorbed on the support accepting one electron each, from Nb. This in turn helps Nb to attain the most preferred charge state, +5. A careful observation of the Fermi-level position (blue dashed line) in DOS plots reveals that the Fermi level of the system, which was initially near CBM, comes down to the VBM of BaO when all the excess five electrons from Nb are donated to five Au atoms, indicating that the five Au atoms bound on the BaO{001} slab with the subsurface Nb interstitial forms a well-stable system as a whole. Figure 10 depicts the charge density difference plots for the Nb-doped BaO support with varied number of Au atoms; the corresponding iso-value is 0.051. The cyan and yellow contours refer to depletion and accumulation of charges around the atoms, respectively. This plot further justifies the charge-transfer process between Nb and Au atoms and the continuous depletion of charge on the Nb atom as more Au atoms are added to the support.

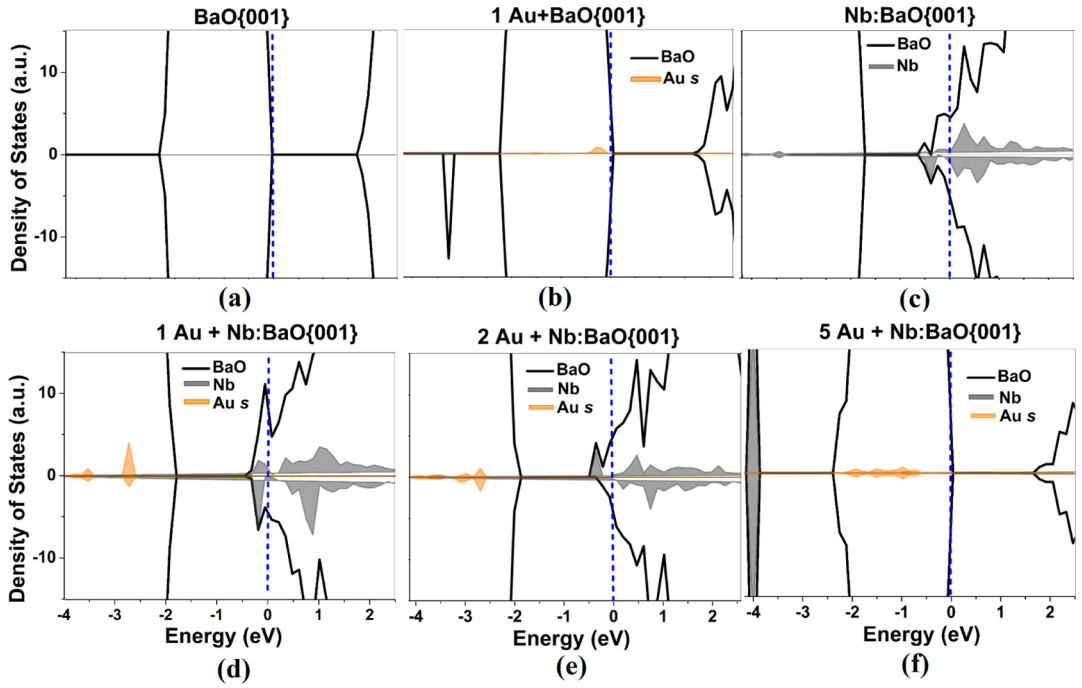

Figure 9. Atom-resolved DOS for (a) pure BaO, (b) one Au atom adsorbed on pure BaO, and (c) Nb-doped BaO{001} surface; (d) one Au, (e) two Au, and (f) five Au atoms adsorbed on the Nb-doped BaO{001} surface. For Au, only 6s states are shown. The blue dashed line indicates the Fermi level.

https://doi.org/10.1021/acs.jpcc.1c07859
J. Phys. Chem. C XXXX, XXX, XXX−XXX

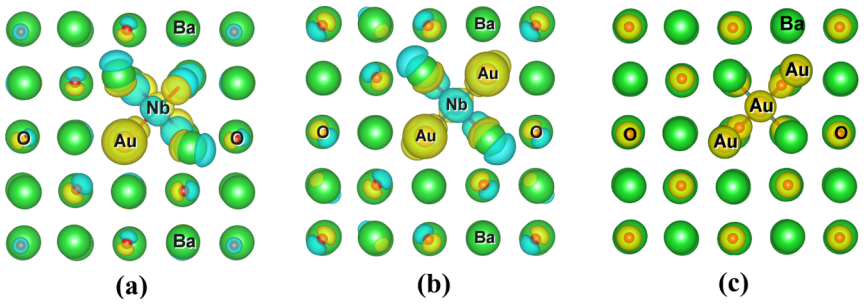

Figure 10. Charge density difference plots for (a) one Au atom, (b) two Au atoms, and (c) three Au atoms adsorbed on the Nb-doped BaO{001} surface. Cyan and yellow contours refer to depletion and accumulation of charges around the atoms, respectively.

DISCUSSION

The charge transfer from a substitutional dopant to an adsorbate for stabilizing a single atom of Au has been reported earlier.[12] However, two factors limit their effectiveness in charge transfer, as noted by Stavale et al.:[15] (1) change in the charge state of a substitutionally doped TM in the host and (2) the electron that is to be transferred to the adsorbate can also get captured by the cationic vacancies or morphological defects in the doped oxide. Our approach mitigates these limitations. Nb doped at the substitutional site in BaO would be able to transfer three electrons, while at the interstitial site, it will be able to transfer five electrons. As implantation can be done on single-crystalline BaO, creation of cationic vacancies or morphological defects could be minimized.

To our surprise, the stability against segregation of Au when it accepts charge from the doped TM has not been shown in any of the previous studies. Our results explain why formation of a well-dispersed two-dimensional Au layer on Mo-doped CaO is favorable, as charge gets transferred from Mo to Au, while in the case of Cr-doped MgO, a 3D island of Au is formed, as Cr could not transfer any charge to Au.[15]

Based on our calculations, we propose following the experimental steps to achieve a well-bound single-atom Au on Nb-doped BaO. First, a single layer of Au can be dispersed on the {001} surface of single-crystal BaO, followed by implantation of Nb ions into the BaO surface. Once Nb gets doped into BaO at the subsurface layer, it transfers charge to Au and binds few of those gold SAs on the near-Nb surface oxygen sites of BaO. The loosely bound Au could be washed away, leaving only strongly bound single Au atoms.

CONCLUSIONS

Based on first-principles calculations, we propose a new way to form single-atom Au supported on BaO. We show that such charged Au atoms are also stable against agglomeration, which explains already reported formation of a 2D gold layer on Mo-doped CaO. To achieve such well-dispersed Au, Nb needs to be implanted in BaO, which is stable at the interstitial site in BaO. This process of stabilizing Au on an oxide support provides a distinct advantage over the known methods involving substitutional doping of oxide with TMs using conventional chemical routes. The TM at the interstitial site transfers more charge to the adsorbate on the oxide surface. Also, ion implantation provides area- and concentration-controlled doping as it is a well-established doping route in electronic industries to create n- and p-type semiconductors. Although our results deal with Nb-doped BaO for binding Au single atoms, it opens up the possibility to explore other combinations of oxides doped with different TMs to bind noble metal single atoms.

AUTHOR INFORMATION

Corresponding Author

Debolina Misra − *Department of Physics, Indian Institute of Information Technology, Design and Manufacturing, Kancheepuram, Chennai 600 127, India;* orcid.org/0000-0002-1893-2071; Email: debolinam@iiitdm.ac.in

Author

Satyesh K. Yadav − *Department of Metallurgical and Materials Engineering and Center for Atomistic Modelling and Materials Design, Indian Institute of Technology Madras, Chennai 600 036, India*

Complete contact information is available at: https://pubs.acs.org/10.1021/acs.jpcc.1c07859

Notes

The authors declare no competing financial interest.

ACKNOWLEDGMENTS

The authors thank HPCE, IIT Madras, for providing the computational facility and acknowledge Dr. Somnath Bhattacharya's help for providing access to the VASP source code. This work is not financially supported by any funding agency.

REFERENCES

(1) Liu, J. Catalysis by Supported Single Metal Atoms. *ACS Catal.* **2017**, *7*, 34−59.

(2) Bruix, A.; et al. Back Cover: Maximum Noble-Metal Efficiency in Catalytic Materials: Atomically Dispersed Surface Platinum (Angew. Chem. Int. Ed. 39/2014). *Angew. Chem., Int. Ed.* **2014**, *53*, 10546.

(3) Zhang, J.; Zhao, Y.; Zhao, X.; Liu, Z.; Chen, W. Porous Perovskite LaNiO3 Nanocubes as Cathode Catalysts for Li-O2 Batteries with Low Charge Potential. *Sci. Rep.* **2014**, *4*, 6005.

(4) Cheng, N.; Stambula, S.; Wang, D.; Banis, M. N.; Liu, J.; Riese, A.; Xiao, B.; Li, R.; Sham, T.-K.; Liu, L. M.; Botton, G. A.; Sun, X. Platinum single-atom and cluster catalysis of the hydrogen evolution reaction. *Nat. Commun.* **2016**, *7*, 13638.

(5) Yang, X.-F.; Wang, A.; Qiao, B.; Li, J.; Liu, J.; Zhang, T. Single-Atom Catalysts: A New Frontier in Heterogeneous Catalysis. *Acc. Chem. Res.* **2013**, *46*, 1740−1748.

(6) Sun, S.; et al. Single-atom Catalysis Using Pt/Graphene Achieved through Atomic Layer Deposition. *Sci. Rep.* **2013**, *3*, 1775.

(7) Qiao, B.; Wang, A.; Yang, X.; Allard, L. F.; Jiang, Z.; Cui, Y.; Liu, J.; Jun, L.; Zhang, T. Single-atom catalysis of CO oxidation using Pt_1/FeO_x. *Nat. Chem.* **2011**, *3*, 634.

(8) Jones, J.; Xiong, H.; DeLaRiva, A. T.; Peterson, E. J.; Pham, H.; Challa, S. R.; Qi, G.; Oh, S.; Wiebenga, M. H.; Pereira Hernández, X.

I.; Wang, Y.; Datye, A. K. Thermally stable single-atom platinum-on-ceria catalysts via atom trapping. *Science* **2016**, *353*, 150−154.
(9) Liu, J.-C.; Wang, Y.-G.; Li, J. Toward Rational Design of Oxide-Supported Single-Atom Catalysts: Atomic Dispersion of Gold on Ceria. *J. Am. Chem. Soc.* **2017**, *139*, 6190−6199.
(10) Chen, X. F.; Yan, J. M.; Jiang, Q. Single Layer of Polymeric Metal−Phthalocyanine: Promising Substrate to Realize Single Pt Atom Catalyst with Uniform Distribution. *J. Phys. Chem. C* **2014**, *118*, 2122−2128.
(11) Shao, X.; Prada, S.; Giordano, L.; Pacchioni, G.; Nilius, N.; Freund, H.-J. Tailoring the Shape of Metal Ad-Particles by Doping the Oxide Support. *Angew. Chem., Int. Ed.* **2011**, *50*, 11525−11527.
(12) Prada, S.; Giordano, L.; Pacchioni, G. Charging of Gold Atoms on Doped MgO and CaO: Identifying the Key Parameters by DFT Calculations. *J. Phys. Chem. C* **2013**, *117*, 9943−9951.
(13) Sterrer, M.; Risse, T.; Heyde, M.; Rust, H.-P.; Freund, H.-J. Crossover from Three-Dimensional to Two-Dimensional Geometries of Au Nanostructures on Thin MgO(001) Films: A Confirmation of Theoretical Predictions. *Phys. Rev. Lett.* **2007**, *98*, 206103.
(14) Ricci, D.; Bongiorno, A.; Pacchioni, G.; Landman, U. Bonding Trends and Dimensionality Crossover of Gold Nanoclusters on Metal-Supported MgO Thin Films. *Phys. Rev. Lett.* **2006**, *97*, 036106.
(15) Stavale, F.; Shao, X.; Nilius, N.; Freund, H.-J.; Prada, S.; Giordano, L.; Pacchioni, G. Donor Characteristics of Transition-Metal-Doped Oxides: Cr-Doped MgO versus Mo-Doped CaO. *J. Am. Chem. Soc.* **2012**, *134*, 11380−11383.
(16) Blöchl, P. E. Projector augmented-wave method. *Phys. Rev. B* **1994**, *50*, 17953.
(17) Kresse, G.; Furthmüller, J. Efficient iterative schemes for ab initio total-energy calculations using a plane-wave basis set. *Phys. Rev. B* **1996**, *54*, 11169.
(18) Kresse, G.; Furthmüller, J. Efficiency of ab-initio total energy calculations for metals and semiconductors using a plane-wave basis set. *Comput. Mater. Sci.* **1996**, *6*, 15−50.
(19) Perdew, J. P.; Burke, K.; Ernzerhof, M. Generalized gradient approximation made simple. *Phys. Rev. Lett.* **1996**, *77*, 3865.
(20) Blöchl, P. E.; Jepsen, O.; Andersen, O. K. Improved tetrahedron method for Brillouin-zone integrations. *Phys. Rev. B* **1994**, *49*, 16223−16233.
(21) Misra, D.; Yadav, S. K. Prediction of Site Preference of Implanted Transition Metal Dopants in Rock-salt Oxides. *Sci. Rep.* **2019**, *9*, 12593.
(22) Ramprasad, R.; Zhu, H.; Rinke, P.; Scheffler, M. New Perspective on Formation Energies and Energy Levels of Point Defects in Nonmetals. *Phys. Rev. Lett.* **2012**, *108*, 066404.
(23) Freysoldt, C.; Lange, B.; Neugebauer, J.; Yan, Q.; Lyons, J. L.; Janotti, A.; Van de Walle, C. G. Electron and chemical reservoir corrections for point-defect formation energies. *Phys. Rev. B* **2016**, *93*, 165206.
(24) Freysoldt, C.; Grabowski, B.; Hickel, T.; Neugebauer, J.; Kresse, G.; Janotti, A.; Van de Walle, C. G. First-principles calculations for point defects in solids. *Rev. Mod. Phys.* **2014**, *86*, 253−305.
(25) Bajaj, S.; Pomrehn, G. S.; Doak, J. W.; Gierlotka, W.; Wu, H.-j.; Chen, S.-W.; Wolverton, C.; Goddard, W. A.; Jeffrey Snyder, G. Ab initio study of intrinsic point defects in PbTe: an insight into phase stability. *Acta Mater.* **2015**, *92*, 72−80.
(26) Van de Walle, C. G.; Neugebauer, J. First-principles calculations for defects and impurities: Applications to III-nitrides. *J. Appl. Phys.* **2004**, *95*, 3851−3879.
(27) Massih, A. R.; Pérez, R. J. *Thermodynamic Evaluation of the Nb−O System*; Quantum Technologies AB, 2006.
(28) Bader, R. F. *Atoms in Molecules*; Wiley Online Library, 1990.
(29) Sanvile, E.; Kenny, S. D.; Smith, R.; Henkelman, G. Improved grid-based algorithm for Bader charge allocation. *J. Comput. Chem.* **2007**, *28*, 899−908.
(30) Tang, W.; Sanville, E.; Henkelman, G. A grid-based Bader analysis algorithm without lattice bias. *J. Phys.: Condens. Matter* **2009**, *21*, 084204.
(31) Zeng, C.; Chen, Y.; Liu, C.; Nobusada, K.; L Rosi, N.; Ji, R. Gold Tetrahedra Coil Up: Kekulé-Like and Double Helical Superstructures. *Sci. Adv.* **2015**, *1*, No. e1500425.
(32) Li, F.; Tang, Q. An Au22(L8)6 nanocluster with in situ uncoordinated Au as a highly active catalyst for O2 activation and CO oxidation. *Phys. Chem. Chem. Phys.* **2019**, *21*, 20144−20150.
(33) Häkkinen, H.; Landman, U. Gold clusters (AuN,2 ≤ N ≤ 10)and their anions. *Phys. Rev. B* **2000**, *62*, R2287−R2290.
(34) Zanti, G.; Peeters, D. Electronic structure analysis of small gold clusters Aum(m≤ 16)by density functional theory. *Theor. Chem. Acc.* **2012**, *132*, 1300.

https://doi.org/10.1021/acs.jpcc.1c07859
J. Phys. Chem. C XXXX, XXX, XXX−XXX